A&A 415, 171–177 (2004)
DOI: 10.1051/0004-6361:20034612

Astronomy & Astrophysics

Dust and dark gamma-ray bursts: Mutual implications

S. D. Vergani[1], E. Molinari[1], F. M. Zerbi[1], and G. Chincarini[2]

[1] INAF-Osservatorio Astronomico di Brera, via Bianchi 46, 23807 Merate (Lc), Italy
[2] Università di Milano Bicocca, Piazza della Scienza 3, 20126 Milano, Italy

Received 27 March 2003 / Accepted 9 October 2003

Abstract. In a cosmological context dust has been always poorly understood. This is true also for the statistics of Gamma-Ray Bursts (GRBs). We therefore started a program to understand the role of dust both in GRBs and as function of z.
This paper presents a composite model that considers a rather generic distribution of dust in a spiral galaxy and considers the effect of changing some of the parameters characterizing the dust grains, size in particular. We first simulated 500 GRBs distributed as the host galaxy mass distribution, using as a model the Milky Way. If we consider dust with the same properties as those we observe in the Milky Way, we find that due to absorption we miss ~10% of the afterglows assuming we observe the event within 100 s–1 hr.
In our second set of simulations we placed GRBs randomly inside giant molecular clouds, considering different kinds of dust inside and outside the host cloud and the effect of dust sublimation caused by the GRB inside the clouds. In this case absorption is mainly due to the host cloud and the physical properties of dust play a strong role. Computations from this model agree with the hypothesis of host galaxies with an extinction curve similar to that of the Small Magellanic Cloud, but the host cloud could be characterized also by dust with larger grains. Unfortunately, the present statistics lack significance, being based on incompatible observations, at different times from the burst and with different limiting magnitudes. To confirm our findings we need a set of homogeneous infrared observations. The use of forthcoming dedicated infrared telescopes, like REM, will provide a wealth of new afterglow observations.

Key words. gamma rays: bursts – ISM: dust, extinction

1. Introduction

Observations show that about 50% of detected GRBs are not visible in optical wavelengths. Statistics refers to well localized bursts (Bloom et al. 2002) with an X ray flux rather similar to those that have been detected also in the optical band. The rapid decline of the optical afterglow (Fynbo et al. 2002; Berger et al. 2002) cannot explain the observations and thus we call them dark bursts.

In two cases, GRB 970828 and GRB 990506, in spite of lacking the optical afterglow we were able to identify the host galaxies ($z = 0.958$ and $z = 1.3$ respectively) so that in these cases it is evident that high redshift is not the cause of the optical flux extinction. A possible explanation is that the events have been obscured by dust. After the first part of our work was completed (Vergani 2002), Reichart (2001) and Reichart & Price (2002) made a case for a strong absorption occurring in the molecular clouds where the event originates. This is in agreement with the current thinking that GRBs are related to massive star formation which is strongly correlated with very dusty regions. Whether we are dealing with a particular type of galaxy is not known. Ramirez-Ruiz et al. (2002) assert that we might be dealing with ULIRG (Ultra Luminous Infrared Galaxies) or similar objects and that the extinction is essentially due to the dust distribution present in these galaxies. We do not have observational evidence that this is the case however. We must also account for the local process of dust sublimation and understand how much dust a burst is capable of sublimating and sweeping out.

We decided to tackle the problem first theoretically, and this paper reports part of our work in this direction. We also proceeded observationally by building the robotic NIR Telescope REM (Zerbi et al. 2002; Chincarini et al. 2003). The statistics of GRBs will increase when the Swift satellite is launched (Gehrels et al. 2003).

In Sect. 2 we discuss how we model the dust, Sect. 3 is devoted to the construction of the simple host galaxy; a basic GRB distribution model and results are presented in Sect. 4. In Sects. 5 and 6 we associate GRBs with giant molecular clouds and we explore its implications. Conclusions are drawn in Sect. 7.

2. Dust model

The afterglow radiation reaches the observer after interacting with circumburst material, host ISM, IGM and the ISM of our

Send offprint requests to: S. D. Vergani,
e-mail: vergani@merate.mi.astro.it

Table 1. Physical characteristics of H_2 galactic clouds.

(1)	(2)	(3)	(4)	(5)	(6)	(7)
	R	n_H	No.(bulge)	No.(disk)	Unit mass	Total mass
GMC	20	5×10^2	800	4000	4×10^5	1.92×10^9
DC	2	5×10^4	16 000	80 000	5×10^3	4.8×10^8

Radius is in pc and n_H in cm^{-3}. Masses are in $M_\odot$.

galaxy. In this work we consider only the interaction with the dust in the ISM of the host galaxy.

Our dust model is based on the Mathis et al. (1977) model, improved by Mathis (1986). We suppose that dust is made up of spherical grains composed 50% of graphite and 50% of silicates with a grain size a distributed as

$$n(a) = n_0 a^{-3.5} \quad (1)$$

with $a_{min} = 0.005\ \mu$m, $a_{max} = 0.25\ \mu$m and n_0, proportional to the neutral hydrogen density ($n_H[cm^{-3}]$), used by Venemans & Blain (2001).

The variation in magnitudes produced after interaction with dust grains is

$$\Delta m \propto \int_0^\infty Q_{ext} \pi a^2 n(a) da \quad (2)$$

with Q_{ext} = extinction efficiency (sum of scattering and absorption efficiency, see van de Hulst 1957).

By varying the fraction of the two types of materials in our model, the exponent of the grain size distribution and the grain size, the result is a change in the scale of the curve without modifying its shape. We cannot therefore disentangle their contribution from different hydrogen column densities ($NH[cm^{-2}]$) along the line of sight. The size of the grains play a strong role. Large grains, which could be present in regions with intense star formation (Maiolino et al. 2001) or in the circumburst environment after the burst has sublimated the smaller grains (Venemans & Blain), cause the extinction curve to flatten. For dust composed only of large grains ($a_{min} = 1\ \mu$m, $a_{max} = 2\ \mu$m) our computations predict a fixed value of $\Delta m \sim 0.1$, in agreement with the theory, that predict for the case $2a > \lambda$ a fixed value of $Q_{ext} \sim 2$ (Fig. 1). The effects of modifying a_{min} with fixed a_{max} are not relevant.

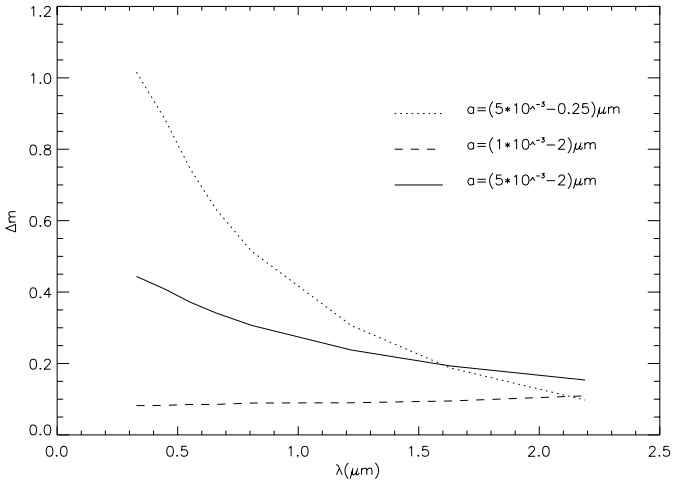

Fig. 1. Extinction curves produced by varying the dust grain size in case of hydrogen column density of 10^{21} cm^{-2}. The dotted steeper curve represents the extinction considering our Galaxy-like dust model (STD, see Table 4) based on Mathis (1986). Dashed and solid lines describe the extinction curve in the case of a dust composed of larger grains (OLG and LRG, respectively).

3. Galactic-like model

We model host galaxy similar to our Milky Way, where the dust is distributed as the neutral hydrogen, both molecular (H_2) and atomic (HI).

For the galactic hydrogen surface density we adopt the values taken from Scoville (1992), and Binney & Merrifield (1998).

For H_2, two Gaussian fits were drawn on nuclear and disk data: namely the gas density has been expressed as:

$$NH(\text{bulge}) \propto e^{\frac{-R^2}{2(0.28)^2}} cm^{-2} \quad (3)$$

and

$$NH(\text{disk}) \propto e^{\frac{-(R-5.03)^2}{2(1.8)^2}} cm^{-2} \quad (4)$$

for the bulge and the disk, where R is the radial distance in cylindrical coordinates (kpc). The total mass of galactic H_2 is distributed with $4 \times 10^8\ M_\odot$ in the bulge and $2 \times 10^9\ M_\odot$ in the disk. The H_2 clouds are present in two distinct morphologies, which we catalogue as giant molecular clouds (GMC) and dense clouds (DC) whose adopted characteristics are summarized in Table 1. An algorithm assigns positions, with a random distribution weighted by Galaxy mass density, to GMC and DC.

Neutral atomic hydrogen is present in a diffuse form throughout the disk system with a total mass of $4.3 \times 10^9\ M_\odot$. Following Binney & Merrifield (1998), we simplify its distribution as being sharply confined in the radial interval $3 < R < 18$ (R in kpc) with a spatial density represented by $n_H[cm^{-3}] = 0.797 e^{-h^2/0.02}$ (where h is the height from Galactic plane in kpc). In Fig. 2 we plot the adopted fits for HI (dashed line) and H_2 (solid lines) surface densities, while Fig. 3 shows the appearance of the host galaxy hydrogen distribution.

4. Basic GRB absorption model

We suppose that the GRBs are distributed as the luminosity (barionic mass) of the host Milky Way-like galaxy. Using the Milky Way photometric model of Kent et al. (1991), we have

$$j_d(R,h) = \frac{I_d}{2h_0} e^{-R/R_d - |h|/h_0}, \quad (5)$$

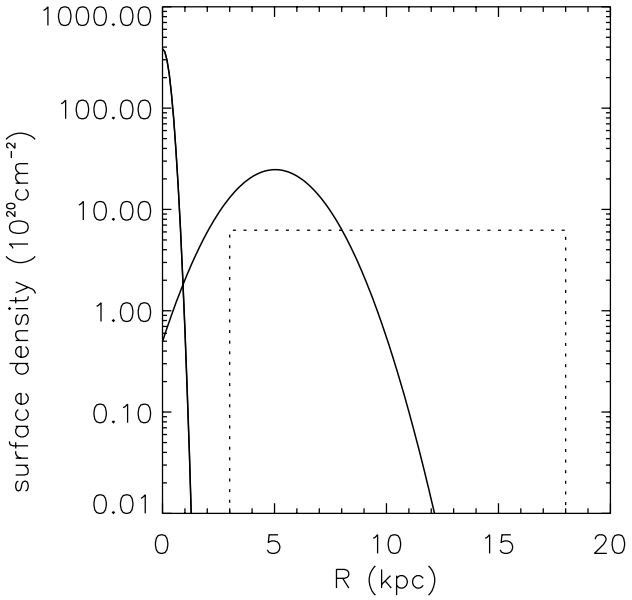

Fig. 2. Milky Way hydrogen column density as a function of radial distance R in kpc. The two solid curves are the two Gaussian fits to the distribution reported in Scoville (1992), for the molecular hydrogen (H_2). The dashed line is the atomic hydrogen (HI) surface density, simplified as a box function between 3 and 18 kpc from galactic center.

with

$$h_0 = \left[0.165 + 0.21\left(R/R_0 - \frac{5}{8}\right)\right] \text{kpc}, \quad (6)$$

$R_\mathrm{d} = 3$ kpc, $R_0 = 8$ kpc and the central surface brightness $I_\mathrm{d} = 1000\ L_\odot\ \mathrm{pc}^{-2}$.

The bulge has been modeled using a King profile

$$I(r) \propto [1 + (r/r_\mathrm{c})^2]^{-3/2} \quad (7)$$

with $r_\mathrm{c} = 0.25$ kpc.

The fraction of GRBs located in the Galactic disk and in the bulge is derived assuming a mass ratio disk to bulge of 4.5.

The burst occurs randomly using as a weighting function the distribution of mass of the galactic model. The observer is located randomly over a 4π solid angle.

Each molecular hydrogen cloud results in absorption and the amount of NH is integrated along the line of sight. The quantized NH amount is then 4.5×10^{22} cm^{-2} for the GMC and 2.25×10^{23} cm^{-2} for the DC.

The atomic diffuse hydrogen is summed integrating along the line of sight from the GRB to a radius of 20 kpc from the galactic center. The HI contribution ranges therefore from a null value to 7×10^{22} cm^{-2}, with a peak at about 5×10^{20} cm^{-2} not sufficient to obscure the afterglow. On the other hand the encounter of a single cloud yields values of NH of about 5×10^{22} cm^{-2} (GMC) or 5×10^{23} cm^{-2} (DC) large enough to completely absorb the optical afterglow.

The total amount of NH is computed and catalogued for the whole 500 GRB set and for the subset of 91 nuclear bursts. In Fig. 4 the histogram of the total NH distribution is shown for the two populations. To better appreciate the difference a cumulative distribution for a smaller range of column densities is reported.

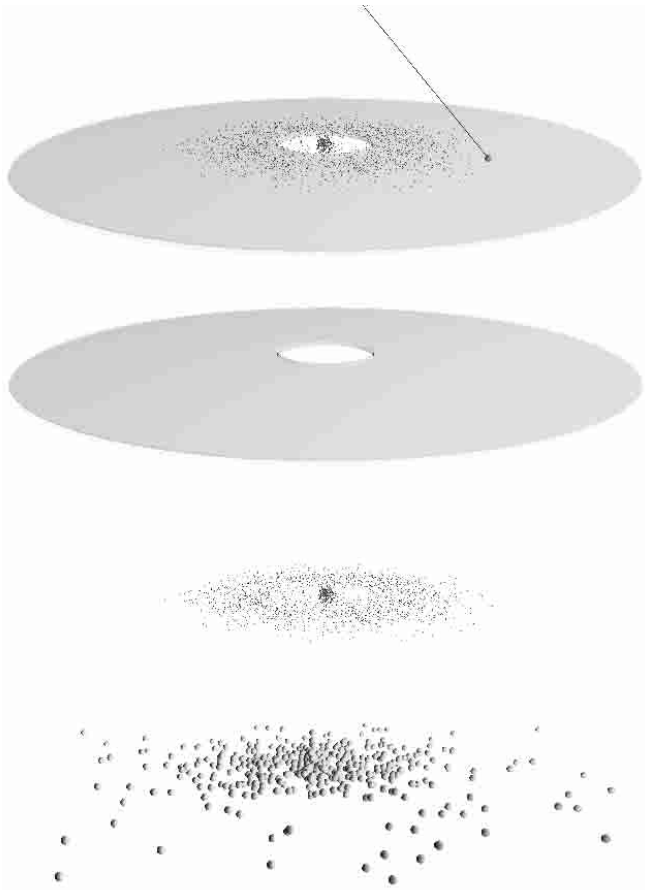

Fig. 3. A rendered image of our host galaxy model. The top figure is the complete model with the sphere on the right which represents a randomly positioned GRB. Its line of sight crosses the galactic plane. Below the distribution of the atomic hydrogen (HI) and H_2 clouds (both GMC and DC) are separately shown. In the bottom picture we present the simulated distribution of the 500 GRBs.

The amount of dark GRBs due to dust absorption can now be estimated, once we have fixed the limiting magnitude of our telescopes in the various passbands and the typical apparent magnitude of GRB afterglows. We randomly associate to each GRB a jet opening angle θ following the law $\propto\theta^{-0.85}$ that we have extrapolated from the known jet angles reported by Bloom et al. (2003) (see Fig. 7, upper panel). Note that the θ distribution is truncated as $0.05 < \theta[\mathrm{rad}] < 0.6$. Considering the luminosity L proportional to θ^{-2}, we calculate the magnitudes R and K of GRBs at 100 s and 5000 s, taking as reference GRB 990123 shifted at $z = 1$ (that is the observed mean redshift of GRBs, Hurley et al. 2002), the color data by Simon et al. (2001) and using the relation

$$m_{GRB} = m_{990123} + 5\log(\theta/\theta_{990123}) \quad (8)$$

where θ_{990123} and m_{990123} are the jet angle and the magnitudes of GRB 990123. To compute the limiting magnitudes we assume use of the REM telescope for the fast response to the GRB alert in R and K bands, and the FORS and ISAAC camera of ESO/VLT for the long term observations (Table 2).

For each GRB we calculate the extinction in R and K caused by the traversed NH column density. We are then able

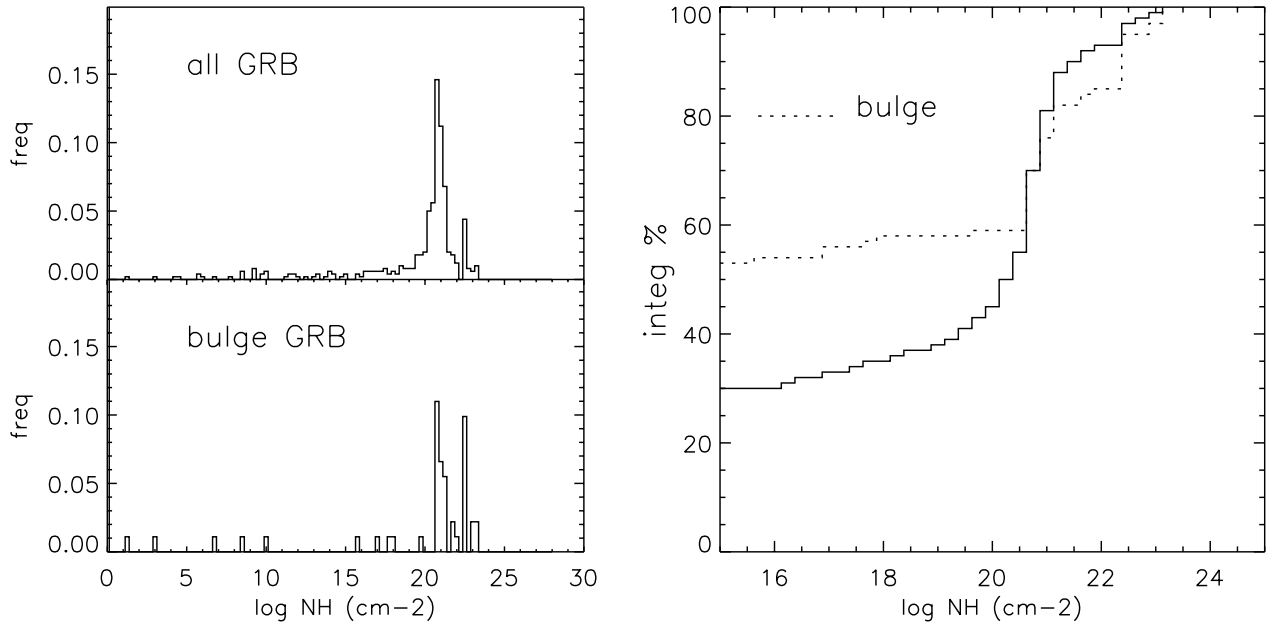

Fig. 4. Hydrogen column density distribution for 500 simulated GRBs.

Table 2. Extinction limits computed on the basis of the limiting magnitudes of different instruments and of GRB990123 afterglow light curve. *NH* values are computed using the dust model in Sect. 2.

(1)	(2)	(3)	(4)	(5)	(6)	(7)	(8)	(9)	(10)
	s	m_R	m_K	$R_{\rm lim}$	$K_{\rm lim}$	A_R	A_K	NH_R	NH_K
prompt	100	10	7.5	19	15.5	9	8	0.86	2.13
late	5000	16	13.5	24	20.5	8	7	0.76	1.87

(3) (4) In these columns are reported light curve values GRB990123-like.
(5) (6) Prompt observation simulated with REM (Vergani 2002, Table 2.3), late observation simulated with ISAAC and FORS (see `http://www.eso.org/oserving/etc/` for its ETC time estimates).
(9) (10) in units of 10^{22} cm^{-2}.

Table 3. Optical (R) and infrared (K) transient loss (%). Prompt and late observation cases are reported for z=1 galaxy position.

	(1)	(2)	(3)	(4)	(5)
		% lost of all GRBs		% lost of bulge GRBs	
		R	K	R	K
$z = 1$	prompt	9	7	18	14
	late	9	7	18	14

to compute the percentage of lost afterglows due to dust absorption under the assumption that the host galaxy at $z = 1$ has dust properties similar to Milky Way.

In Table 2 R and K magnitudes of prompt and late observations for GRB 990123-like events are reported. The values of NH quoted in Cols. (9) and (10) represent the computed amount of NH needed, according to our dust model, to obtain the extinction values of Cols. (7) and (8). The summary of Table 3 is a clear indication that only a relatively small fraction of GRBs is *not* observed due to dust extinction in the case of a host galaxy at $z = 1$.

5. GRBs in molecular clouds

Our results show that, if the GRB distribution is similar to the mass distribution and if the dust of the host galaxies has the same characteristics as Galactic dust, the percentage of dark GRBs due to dust obscuring is rather low. There is no relevant difference between R and K observations and between percentages relative to observations taken at 100 s and 5000 s. It also happens that no burst, out of the 500 considered, occurs statistically inside a molecular cloud. In this scenario the majority of dark bursts could be due to high redshift Ly-α absorption.

We then consider the case where GRBs follow the distribution of giant molecular clouds. Physically the assumption is that of a strong connection between GRBs and massive star formation.

Within this framework, we place 5000 GRBs inside our modeled giant molecular clouds that have similar characteristics to the supposed typical GMC GRB host described by Galama & Wijers (2001).

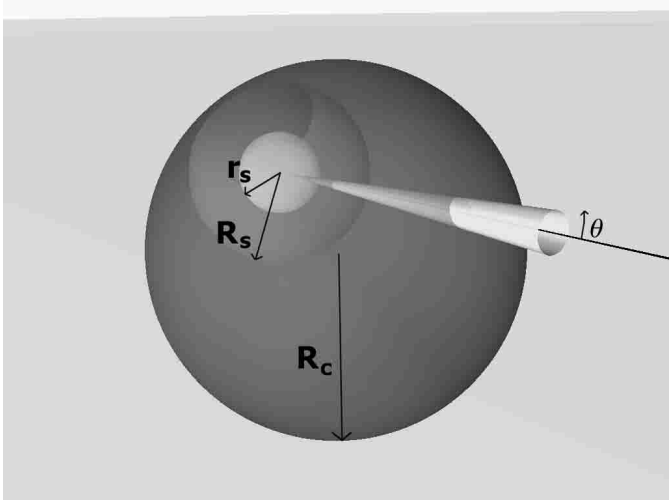

Fig. 5. Geometry around the GRB location explaining the shapes of the four regions whose content in terms of dust is parameterized in our models. The regions are spherical shells centered on the GRB location delimited by r_s (the radius up to which all dust grains are destroyed), R_s (the radius up to which grains with radius smaller 1 μm are destroyed), R_C (the radius of the giant molecular cloud) and the border of the galaxy. θ is the jet opening angle associated with the GRB event.

The first aspect to consider is dust sublimation by the optical-UV flash accompanying the GRB, a phenomenon likely confirmed by the observations of the afterglow light curve of GRB 990123 (Akerlof et al. 1999). We consider the results of Waxman & Draine (2000) and Reichart (2001b) that compute the radius up to which the dust is sublimated, which is also a function of dust grain size. In the case of a canonical distribution of graphite and silicate grain size, the sublimation radius is $R_s \simeq 10\, L_{49}^{1/2}$ pc where L_{49} is the 1–7.5 eV (1600–12 000 Å) isotropic-equivalent peak luminosity of the optical flash in units of 10^{49} erg s^{-1}, that is, the 1–7.5 eV isotropic-equivalent peak luminosity of the optical flash of GRB 990123.

Inside the host cloud we consider both the case of standard galactic dust and the case of dust, already present before the sublimation took place, with larger grain size with $a_{\rm min} = 0.005$ μm, $a_{\rm max} = 2$ μm, because of the connection of GRBs and intense star formation regions (Galama & Wijers 2001), as described in Sect. 2. Moreover, in the case of large grains, we have to consider two different sublimation radii: an inner one (r_s) up to which all grains are destroyed and a larger one (R_s) up to which only the grains whit a radius smaller than 1 μm can be sublimated (Venemans & Blain).

R_s and r_s vary with the intensity of the peak luminosity of the optical flash, that we can suppose depends on the GRB jet opening angle θ. We calculate for each GRB R_s and r_s as $R_s = R_{s990123} * \theta_{990123}/\theta$ and $r_s = r_{s990123} * \theta_{990123}/\theta$, where $R_{s990123}$, $r_{s990123}$ and θ_{990123} are the two sublimation radii and the jet opening angle of GRB 990123.

To each of the 5000 simulated GRBs is associated a random line of sight passing through 4 regions: $\Re 1$ is the inner region from the GRB to r_s (the radius up to which all dust grains are destroyed); $\Re 2$ goes from r_s to R_s, where large grains (radii from 1 μm to 2 μm) are allowed to survive; $\Re 3$ is the rest of the undisturbed host cloud dust; $\Re 4$ is the host galaxy outside the host cloud, consisting of all other molecular clouds and of the diffuse medium (see Fig. 5). In these regions we place 5 kinds of dust yielding ten different models.

Table 4. Regions around GRBs and their contents in term of dust type as adopted in our computations. Dust model used are: STD (our model of standard Galactic dust, with grain radii from 0.005 μm to 0.25 μm); LRG (with added larger grains, from 0.005 μm to 2 μm); OLG (only large grains, left from partial sublimation, with radii from 1 μm to 2 μm); GRA (only large graphite grains, left from partial sublimation) SMC (dust with low extinction similar to Small Magellanic Clouds); SUB (no dust, completely sublimated by the burst).

(1)	(2)	(3)	(4)	(5)
	$\Re 1$	$\Re 2$	$\Re 3$	$\Re 4$
model 1	*SUB*	*OLG*	*LRG*	*STD*
model 1b	*SUB*	*GRA*	*LRG*	*STD*
model 2	*SUB*	*SUB*	*STD*	*STD*
model 3	*SUB*	*OLG*	*STD*	*STD*
model 3b	*SUB*	*GRA*	*LRG*	*STD*
model 1smc	*SUB*	*OLG*	*LRG*	*SMC*
model 1smcb	*SUB*	*GRA*	*LRG*	*SMC*
model 2smc	*SUB*	*SUB*	*SMC*	*SMC*
model 3smc	*SUB*	*OLG*	*SMC*	*SMC*
model 3smcb	*SUB*	*GRA*	*SMC*	*SMC*

In the first three models, to calculate the extinction in the region outside the host molecular clouds, we use our Galactic-like dust model. In $\Re 3$, the part inside the host molecular clouds where there is no sublimation, 2 scenarios are explored: standard galactic dust (model 2 and 3) or a similar one but with larger grains ($a_{\rm max} = 2$ μm, model 1). In model 2 we suppose that dust in the whole cloud is standard and thus sublimated both in $\Re 1$ and $\Re 2$, whereas in model 1 and 3 the circumburst medium is supposed to be characterized by dust with $a_{\rm max} = 2$ μm, thus in $\Re 2$ dust grains larger than 1 μm are left.

Hyorth et al. (2003) have recently supported the hypothesis that GRB environments have an extinction curve similar to that of the Small Magellanic Cloud (SMC), so, in model 1smc, 2smc and 3smc we present the same scenario of model 1, 2 and n 3 but considering SMC extinction inside the cloud and/or in the host galaxy. Both the cases of extinction caused by larger grains or SMC-like dust agree with the non detection of the $\lambda = 2175$ Å bump (Galama & Wijers 2001), that is instead a significant feature of Galactic-like dust.

Simulations by Perna et al. (2003) show that if we consider dust with properties similar to Galactic, the burst energy very quickly sublimes silicate grains present in the circumburst medium differently from graphite-made grains that need a longer time to be destroyed and whose sublimation is more efficient on smaller grains. On this basis, we think it reasonable to consider models (model 1b, 3b, 1smcb and 3smcb) in which dust in the $\Re 2$ region is composed only of graphite grains with $a_{\rm min} = 1$ μm, $a_{\rm max} = 2$ μm. Table 4 shows all the cases.

6. Results

The percentage of dust-obscured afterglows for each model is computed summing all the absorption intervening in the four

Table 5. Optical (R) and infrared (K) transient loss (%) in the GRB-GMC association scenario. The models are described in the text and Table 4.

(1)	(2)	(3)	(4)	(5)
	R		K	
	prompt	late	prompt	late
model 1	53.0	57.3	38.8	44.8
model 1b	52.8	57.1	38.5	44.5
model 2	67.9	69.8	49.5	54.0
model 3	68.2	70.0	49.9	54.5
model 3b	57.8	57.1	38.5	44.5
model 1smc	46.8	51.1	29.9	36.6
model 1smcb	46.6	50.8	29.4	36.4
model 2smc	7.0	10.4	0.2	0.3
model 3smc	7.2	10.7	0.2	0.4
model 3smcb	7.1	10.6	0.2	0.3

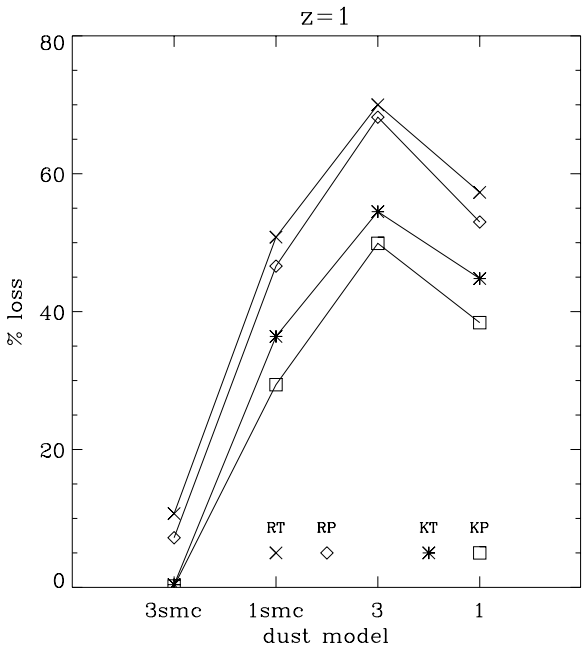

Fig. 6. Trends for the most relevant models of the percentage for prompt (RP, KP) and late (RT, KT) observations in R and K bands of dark bursts caused by dust extinction.

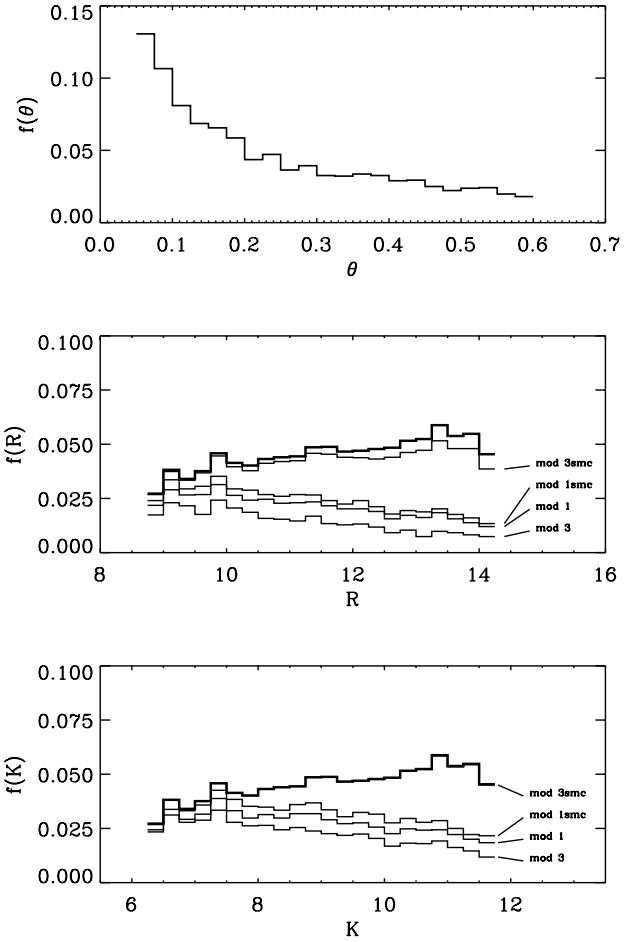

Fig. 7. Distribution of the θ jet opening angles of our 5000 GRB simulated sample (upper panel). The parent distribution follows a $\theta^{-0.85}$ law after a fit to observed jet angles. The middle panel shows the translation of jet angles in R magnitudes (heavy line). The transformation lies on the zero point of a GRB 990123-like event at $z = 1$ ($\theta = 0.086$, $R = 10$, $K = 7.5$) and the assumption of the conservation of the total flux on the emitting solid angle ($\propto\theta^2$). Thinner lines are the luminosity function of the early observed (non-absorbed in our simulations) afterglows in the R band. The four histograms refer to different models: 1, 3, 1smc and 3smc. In the lower panel the same set of distributions are plotted for the K filter (note that model 3smc does not differ from the original distribution, plotted as a heavy line).

regions. Critical limiting magnitudes, beyond which the transient is no longer visible, are taken from Cols. (5) and (6) of Table 2 while extinction curves used for standard Galactic dust and larger grain dust are respectively the dotted and the solid ones represented in Fig. 1. For the SMC extinction curve we use the one reported by Weingartner & Draine (2001).

If in $\Re 2$ there are only grains larger than 2 μm (both in the case of standard and graphite only grains) we use the dashed curve of Fig. 1, but multiplied respectively by a factor $F_1 = \int_1^2 a^{-0.5}\mathrm{d}a / \int_{0.005}^2 a^{-0.5}\mathrm{d}a$ and $F_2 = 0.5 * F_1$ taking into account that total dust mass is decreased. The 0.5 factor takes into account that half of the dust population (silicates) has completely disappeared.

In Table 5 results of different models are reported. It is evident that the content in $\Re 2$ is almost not significant, whereas most of the extinction take place in $\Re 3$, so the content of this region has a determining role. In Fig. 6 we plot percentages for relevant cases.

In the lower panels of Fig. 7, we show magnitude distributions (R and K) of the simulated afterglows after 100 s for GRBs at $z = 1$. Together with the complete population, the distributions of observed transients for the different models are plotted.

A comparison of our simulation of Swift and REM data with observations available now would be misleading. From our point of view it is practically impossible to extract a statistically significant number (e.g. % of real dark bursts) from a set of observations performed with different telescopes (i.e. limiting magnitudes) and at different times from the burst. To stress this point we compute at different times the percentage of

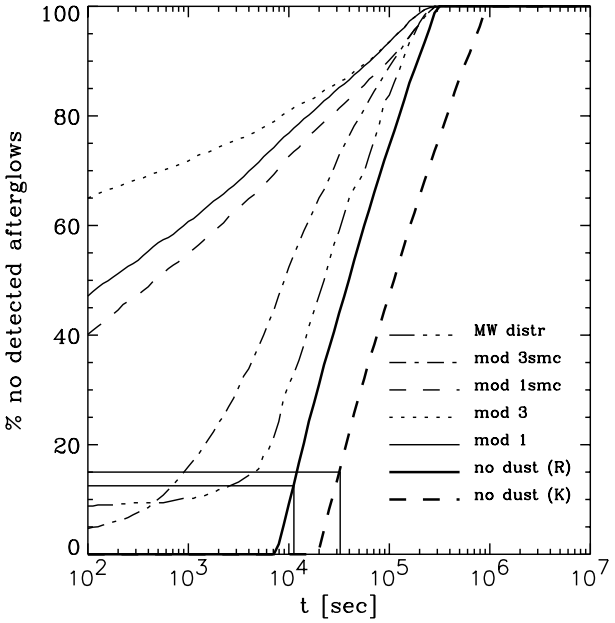

Fig. 8. Percentage of lost afterglows as a function of observing time for GRB at $z = 1$ with our simulated light curves. The solid bold line represents the R band curve without considering dust extinction, $R_{\rm lim} = 21$; dashed bold line represents the K band curve without considering dust extinction, $K_{\rm lim} = 19$, whereas the other curves report R band results from our models calculated for $R_{\rm lim} = 21$. Two line intersections show the percentages in R and K relative to the data of GRB 020819.

events for which the OT would not be observed even without dust extinction, considering the light curves of our simulated GRBs and fixing R limiting magnitude as $R_{\rm lim} = 20.5$. The solid bold line in Fig. 8 shows that for the majority of times of observation the percentage of lost events is significant. The dashed bold line of Fig. 8 reports the computation made for the K infrared transient with $K'_{\rm lim} = 19$.

Recently Klose et al. (2003) dealt with a GRB (GRB 020819) whose afterglow has been searched for without success in K', 0.37 days after the burst down to $K' = 19$ and in R band 0.13 days after the burst down to $R = 20.5$. We report these observational times and magnitudes in Fig. 8: we notice that we cannot exclude that GRB 020819 is not a real obscured or high redshift burst. If the observations reach $R_{\rm lim} = 24$, the value at 0.13 days of the R band curve not affected by dust is null and that late K observations (more than 6 hours after the burst) are always noticeably biased.

We add to Fig. 8 the R band results of our models (i.e. considering extinction) at the same magnitude limit.

7. Conclusions

We have considered different kinds of dust and their role in obscuring optical and NIR afterglows of GRBs simulated with different distributions inside a galaxy at $z = 1$. In the case of GRBs occurring inside giant molecular clouds, our simulations show that dust in GRB host galaxies does not have the same properties as galactic dust, otherwise dark GRBs would be seen more often. Furthermore our results agree with the hypothesis of a dust extinction curve of GRB host galaxies similar to that of the SMC. Moreover, if the host molecular cloud is characterized by large dust grains, high redshift plays a minimal role in the causes of dark GRBs. The opposite holds if the dust inside the host molecular cloud also has SMC properties.

Once we will gather enough early K observations we will be able to estimate the nature of the dust present in host molecular clouds from the fraction of lost K afterglows.

We underline the fact that with present observational data it is impossible to produce real statistics for dark bursts due to the late and varying time of observations and to the different magnitudes reached.

In the future, from the afterglow results given by Swift and REM, we will be able to determine the nature of dark GRBs. Indeed with a further refinement of the model and good statistics of bursts observed in various colors we will be able to know what kind of dust is present in the environment of the burst.

Acknowledgements. The authors want to thank Stefano Covino and Daniele Malesani for the useful discussions.

References

Akerlof, C., Balsano, R., Barthelemy, S., et al. 1999, Nature, 398, 400
Berger, E., Kulkarni, S. R., Bloom, J. S., et al. 2002, ApJ, 581, 981
Binney, J., & Merrifield, M. 1998, in Galactic Astronomy (Princeton University Press), 559, Fig.9.19
Bloom, J. S., Kulkarni, S. R., & Djorgovski, S. G. 2002, ApJ, 123, 1111
Bloom, J. S., Frail, D. A., & Kulkarni, S. R. 2003, ApJ, 594, 674
Chincarini, G., Zerbi, F. M., Antonelli, A., et al. 2003, ESO Messenger, in press
Fynbo, J. U., Jensen, B. L., Gorosabel, J., et al. 2002, A&A, 369, 373
Galama, T., & Wijers, R. A. M. J. 2001, ApJ, 549, L209
Geherels, N., & Swift Team 2002, AAS, 200, 3001
Hjorth, J., Moller, P., Gorosabel, J., et al. 2003, ApJ, in press
Hurley, K., Sari, R., & Djorgovski, S. G. 2002 [astro-ph/0211620]
Kent, S. M., Dame, T. M., & Fazio, G. 1991, ApJ, 378, 131
Klose, S., Henden, A. A., Greiner, J., et al., ApJ, 592, 1025
Maiolino, R., Marconi, A., & Oliva, E. 2001, A&A, 365, 37
Mathis, J. S., Rumple, W., & Nordsieck, K. H. 1977, ApJ, 217, 425
Mathis, J. S. 1986, ApJ, 308, 281
Perna, R., Lazzati, D., & Fiore, F. 2003, ApJ, 585, 775
Ramirez-Ruiz, E., Threntham, N., & Blain, A. W. 2002, MNRAS, 329, 465
Reichart, D. E. 2001a, A&AS, 198, 2708
Reichart, D. E. 2001b, ApJ, submitted [astro-ph/0107546]
Reichart, D. E., & Price, P. A. 2002, ApJ, 565, 174
Scoville, N. Z. 1992, in The Astronomy and Astrophysics Encyclopedia, ed. S. P. Maran, 374, Fig. 1
Simon, V., Hudec, R., Pizzichini, G., & Masetti, N. 2001, A&A, 377, 450
Van de Hulst, H. C. 1957, in Light scattering by small particle (Wiley & Sons)
Venemans, B. P., & Blain, A. W. 2001, MNRAS, 325, 1477
Vergani, S. D. 2002, laurea thesis
Waxman, E., & Draine, B. T. 2000, ApJ, 537, 796
Weingarnter, J. C., & Draine, B. T. 2001, ApJ, 548, 296
Zerbi, F. M., Chincarini, G., Ghisellini, G., et al. 2002, Astron. Nachr., 322, 275